Modeling Hypoxia in the Central Basin of Lake Erie under Potential Phosphorus Load Reduction Scenarios

Daniel K. Rucinski[1], Joseph V. DePinto[1], Dmitry Beletsky[2] Donald Scavia[3]

[1] LimnoTech, 501 Avis Drive, Ann Arbor, MI 48108, USA

[2] Cooperative Institute for Limnology and Ecosystems Research, School of Natural Resources and Environment, University of Michigan, 4840 South State Road, Ann Arbor, MI 48108, USA

[3] Graham Sustainability Institute, University of Michigan, 625 East Liberty Road, Ann Arbor, MI 48193, USA

Abstract

A 1-dimensional (vertical), linked hydrodynamic and eutrophication model that was previously calibrated and corroborated with 19 years (1987-2005) of observations in the central basin of Lake Erie, was applied as part of a group of models capable of forecasting ecosystem responses to altered phosphorus loads to Lake Erie. The results were part of the effort guiding the setting of new phosphorus loading targets in accordance with the Great Lakes Water Quality Agreement. Our analysis demonstrated that while reductions in total phosphorus loads can be expected to reduce hypoxia and chlorophyll-a impairments on average, climate and meteorological variability will result in significant year to year variability. We provide examples for achieving hypothetical water quality goals and relate the required reductions to recent nutrient sources.

Introduction

Lake Erie has a long history of cultural eutrophication (Beeton 1963) and efforts to mitigate the resulting water quality degradation through nutrient load reductions. Annex 3 of the 1978 Great Lakes Water Quality Agreement (GLWQA 1978) enlisted a suite of eutrophication models to help define a target total phosphorus (TP) load of 11,000 metric tonnes per year for Lake Erie, which initially resulted in improvements in water quality and beneficial uses (DePinto et al. 1986). However, in recent decades, the lake has experienced a return to eutrophic conditions, with central basin hypoxia (dissolved oxygen concentration below 2 $mg \cdot l^{-1}$) returning to substantial size and western basin harmful algal blooms returning (Burns et al. 2005, Zhou et al 2013, Scavia et al. 2014). This re-eutrophication of Lake Erie seems to be a result of changes in the structure and function of the lake ecosystem (Heckey et al. 2011; Scavia et al. 2014) and of changes in the dominant source of nutrient loads (agricultural non-point sources) and the form of those loads (increase in fraction of bioavailable phosphorus).

The 2012 revision of the GLWQA (IJC, 2012) calls for revisiting the target loads for the Great Lakes, and a suite of models were used to assist (Scavia, et. al., this issue). The goal was to use existing, scientifically credible models to investigate the influence of external load reductions to Lake Erie. The models that are focused on Lake Erie hypoxia ranged from simple regressions to complex 3-dimensional ecosystem models. As part of that effort, we adapted a previously corroborated 1-dimensional, linked hydrodynamic-eutrophication model (Rucinski, et. al., 2014).

While most of the other models in the effort focused on a single meteorological year, we investigated the effects of a wide range of meteorological conditions from 1987 to 2005, the period for which the model was previously calibrated and corroborated. This allows us to not only investigate the role of the external phosphorus loading, but also the uncertainty in the lake response as a function of weather and associated mixing regimes.

To help guide target loads, eutrophication response indicators and their associated metrics were defined to describe the ecosystem response to varying loading (Scavia et al. this issue). For the central basin of Lake Erie, the hypoxia metrics included hypoxic area and duration, and the phytoplankton biomass metric was chlorophyll-a concentration. Model derived load-response relationships for these metrics were developed to guide what TP load reduction would be required to achieve an ecologically acceptable threshold for each metric.

Using the 1987-2005 observed meteorological conditions to create a set of thermal regimes as drivers of the ecological model, the model produced forecast envelopes representing the mean response and uncertainty associated with meteorological variation. This approach allows us to generate central tendency response curves, and estimate the deviation from that mean due to meteorological conditions. The results indicate that, while one can estimate the projected impact of a load reduction on average, the actual ecological response can deviate significantly in any given year based on the timing and magnitude of the stratification and associated vertical mixing in the lake.

Modeling Approach

Model Structure

A 1-dimensional hypoxia model representing the offshore waters of the central basin (approximately 24 m depth) of Lake Erie was previously developed, linking an external hydrodynamic model with a simplified nutrient-phytoplankton-zooplankton-detritus (NPZD) eutrophication model. The hydrodynamic model, described in Rucinski et al. (2010), provides temperature and associated vertical mixing profiles on an hourly basis for 48 vertical layers (each 0.5m thick). For the purposes of the following analyses, it is important to note that while interannual variation in stratification properties is highly variable over the simulation period, the long-term trend is relatively flat (Figure 1) . Temporal variation in the modeled thermal regimes is described in detail in Rucinski et al. (2010).

The eutrophication portion of the model incorporates phosphorus and carbon loading to the western and central basins, internal phosphorus cycling, carbon cycling (in the form of algal biomass and detritus), algal growth and death, zooplankton grazing, oxygen consumption and production processes, and sediment interactions (Figure 2). The mass balance equations for the model are documented in Rucinski et al. 2014. While oxygen dynamics may also be influenced by benthic filter feeders (e.g., zebra and quagga mussels; Woynarovich 1961), these drivers were not included in this framework.

The model has been corroborated with in-lake data for dissolved oxygen (DO), total phosphorus (TP), dissolved reactive phosphorus (DRP) and chlorophyll a (chl-a) measurements over nineteen years from 1987-2005 (Rucinski et al. 2014). Observations used in the corroboration were from EPA's online database (GLENDA), EPA's Great Lakes National Program Office (GLNPO), Environment Canada's Water Science & Technology Branch (ECWSTB), and the

International Field Years on Lake Erie Program (IFYLE, 2006). Model output was used to relate inputs (TP loading in this case) to outputs (DO and chl-a metrics) as described below, representing both the mean response to a given load and variability caused by variation in meteorological drivers.

In a similar analysis, Rucinski et al. (2014) developed preliminary response curves for several DO metrics (hypolimnion oxygen demand, hypoxia days, hypoxic area, bottom DO) in relation to annual TP and dissolved reactive phosphorus (DRP) loads using the loading time-series observed in 1997. The current effort adapted this approach, using the baseline loading year of 2008 to be consistent with the other models (Scavia et al., this issue).

Sediment Oxygen Demand

Rucinski et al. (2014) found that sediment oxygen demand (SOD) was a substantial contributor to overall oxygen depletion. For example, in model tests, it was found that even after removing all external phosphorus loads, a 67% reduction of SOD was still required to eliminate hypoxia. Therefore it was necessary to estimate the SOD under different future loading scenarios. Because SOD is dependent upon the settling and subsequent decomposition of organic matter, derived primarily from settling phytoplankton production that is in tern driven by nutrient loads, it is logical to assume that reduced loads would eventually lead to reduced SOD. Rucinski et al. (2014) developed a relationship for Lake Erie between steady state SOD and settled organic matter based on Borsuk et al. (2001). That relationship was then extended based on model simulations of the relationship between TP load and the rate of organic matter sedimentation, thus allowing estimates of SOD corresponding to projected changes in phosphorus loads. Assuming SOD is in steady state with nutrient loading, the resulting equation was:

$$SOD = \left(\frac{SOD_{\max} \cdot TP_{load}}{K_{SOD} + TP_{load}} \right)$$

Where:

$SOD_{\max}$ = maximum sediment oxygen demand ($m^{-2} \cdot d^{-1}$),

TP_{load} = annual total phosphorus load (tonnes·$year^{-1}$),

K_{SOD} = half-saturation constant (tonnes·$year^{-1}$).

The values for SOD_{max} and K_{SOD}, obtained by regression, are 0.98 g· $m^{-2} \cdot d^{-1}$ and 3847 tonnes·$year^{-1}$, respectively.

Model Application

Loading Scenarios

The corroborated model (Rucinski et al. 2014) used detailed daily TP and DRP loads to the western and central basins for 1987-2005 (Dolan and McGunagle 2005, Richards and Baker (2002), Richards 2006). To estimate the load to the central basin from the western basin, an

apparent loss rate of 10 $m \cdot yr^{-1}$ (Lesht et al. 1991) was applied to the western basin loads to account for nutrient uptake and sedimentation.

Similarly, daily TP and DRP loadings for the major tributaries were available for several more recent years from Dave Dolan (reported in Scavia et al. 2014). The 2008 loading time-series was used as the common input set in the multiple model effort because the total annual load from this year (10,800 MT) was similar to the current GLWQA target load (11,000 MT). To assess the response to different nutrient loads, global scalars of 0%, 25%, 50%, 75%, 100%, and 125% relative to the 2008 loading time-series for each scenario were applied to all western and central basin sources.

Ecological Indicators and Response Relationships

To evaluate responses to varying TP loads, we focused on two key central basin characteristics: bottom water hypoxia and summer algal blooms. Three metrics were related to bottom water hypoxia: average August-September hypoxic area, average August-September hypolimnetic DO concentration, and the number of hypoxic days calculated for the entire stratified period. To address the relationship between loads and algal blooms, June-August average chlorophyll-a concentration was used as a surrogate for algal biomass.

Because the model is a 1-d representation of the deepest part of the central basin, we used a previously established (Zhou et al. 2013) relationship between bottom-layer DO concentration and hypoxic area in Lake Erie:

$$A = 9.3 \cdot e^{\left(\frac{-DO^2}{7.09}\right)}$$

Where:

A = hypoxic area (10^3 km^2),

DO = hypolimnetic dissolved oxygen ($mg \cdot L^{-1}$).

Rucinski et al. (2014) applied this equation to corroborated model output and demonstrated that the modeled hypoxic area was consistent with observed areas for a wide range of meteorological and loading conditions. It should be noted that the dataset that was used by Zhou et al. (2013) is based on data from 1987-2007, while this effort focuses on a loading time-series representing 2008. However, the total annual load in 2008 (10,800 MT) is within the range of observed loads from 1987-2007.

Results and Discussion

The response of summer averaged chl-a (June-August) to changes in annual TP load to the western and central basins (Figure 3) saturates at around 2 $\mu g \cdot L^{-1}$, with a more linear response at lower loads. The variability due to meteorology is quite small (shown as +/- 1 s.d. error bars) indicating that variation in net algal growth is influenced more by loads than by variation in climate.

The load-response curve for hypoxic area (Figure 4) for the range of loads tested is the lower end of a saturating function. The similar curve developed by Rucinski et al. (2014) approached an asymptote at loads near 20,000 MT, most likely related to physical constraints of the basin. The one standard deviation error bars illustrate the range of hypoxic areas one can expect from variability in the thermal regime that results from varying inter-annual meteorological drivers.

Similar to the load-response curve for hypoxic area, the number of hypoxic days increases with annual TP load (Figure 5). Note that the number of hypoxic days is calculated for the entire duration of stratification, which varies in each of the 19 thermal regimes, but typically lasts from mid-May to early-October.

As expected, summer average (August-September) hypolimnetic DO concentration declines with increasing annual TP phosphorus load (Figure 6), with significant inter-annual variability driven by meteorology. However, the pattern of seasonal evolution of hypoxia (Figure 7) appears consistent among the 19 thermal regimes with onset ranging between mid-July and mid-August.

Uncertainty and Sensitivity Analysis

Meteorological effects - A number of additional simulations were run to assess the relative importance of factors contributing to development of hypoxia. First, we simulated all combinations of the 19 loading rates and 19 thermal stratification patterns from 1987-2005. That is, the daily loading time-series from each year (1987-2005) was applied to each of the 19 meteorological conditions. Using a two-way Analysis of Variance (ANOVA) without replication showed that variation in meteorology (via thermal stratification) explained 8.9 times as much annual variation in the hypoxic area compared to variation in loading. This suggests that the average hypoxic response in the central basin of Lake Erie is relatively predictable for the range of loads observed in the study period, but meteorological forcing functions will cause significant year to year deviations.

In addition to assessing the impact of load magnitude compared to thermal structure, a separate 19x19 matrix of scenarios was created to investigate the impact of load seasonality. For these scenarios, the same magnitude of annual phosphorus load (equal to the 2008 load) was applied in each year; however the timing of the inputs was adjusting to match that of each of the daily load time-series from 1987-2005. A two way ANOVA (without replication) showed that variation in the thermal structure of the lake explained 14.2 times as much variation in hypoxic area compared to the timing, or seasonality, of the load. This analysis suggests that, for the range of load seasonality observed from 1987-2005, the hypoxic response is far more dependent on stratification structure than on the time of nutrient delivery to the system. A similar analysis was performed in Rucinski et al. (2014) which found that the thermal regime explained 5 times as much variation in hypoxia as the load timing did. However, that analysis used a higher baseline loading magnitude (equal to the 1997 load) which resulted in more hypoxia. The greater magnitude of estimated hypoxia likely limited the influence of seasonal variation in the previous study. In both analysis, the thermal regime was found to explain much more of the variation in annual hypoxia than seasonality.

Further, comparing the annual hypoxic response to average depth to the hypolimnion (Figure 8) illustrates the influence of the thickness of the hypolimnion. It is clear that inter-annual variability in the meteorological drivers of the lake thermal regime has a strong influence on

hypoxic response, and thus captures most of the uncertainty for a given load. This underscores the notion that while scenarios representing the average response of the lake to alterations in nutrient loads can be useful guidance for policy, forecasts for any particular year will be dependent on the lake thermal regime.

Western basin load effects - The original configuration of the model accounted for attenuation of the western basin loads using a net apparent TP deposition rate of 10 $m \cdot yr^{-1}$ (Lesht et al. 1991). For comparison, here we also used nutrient and organic carbon loads entering the central basin from the western basin as calculated by the Western Lake Erie Ecosystem Model (WLEEM) (Verhamme, et al., this issue). WLEEM provides daily aggregates of the mass flux crossing the western-central basin boundary. The WLEEM-linked version of the model produced a somewhat greater magnitude of hypoxia for a given total load (Figure 9), indicating that the load from the western basin is likely greater than the load calculated with a 10 $m \cdot yr^{-1}$ net apparent TP loss rate for the Western Basin, especially at higher loading rates.

It is important to note that both versions of our model used the same parameter set as the original version of the model that attenuated the western basin loads at a constant rate. Therefore, it is expected that the differences in loads entering from the western basin would produce a difference in response, as the calibration parameters could be expected to change with different western basin trapping efficiencies. However, the model versions also differ in how the flow is transported from the western to central basin. WLEEM incorporates a full 3-dimensional hydrodynamic model, which allows for short term circulation and retention in the western basin. The original version of our model simply assumed that the sum of the flow from the western basin tributaries entered the central basin, following the observed hydrograph (after accounting for the constant loss). Therefore, differences in simulated responses between the two model versions are not only a result of the calibration parameters, but also due to different flow hydrographs in the load inputs.

Load sources - Reaching a load reduction that can on average achieve desired improvements in ecosystem health will likely require significant targeted land use management practices and potentially improvements at industrial and municipal treatment plants. The distribution of the TP load from major tributaries to the western basin over several recent years (Dolan, personal communication; IJC 2014), demonstrates that the contribution from the Maumee and Detroit Rivers make up the vast majority of the total western basin load (Figure 10). However, river discharge dictates which is the dominant load in a given year because the Maumee River load has large inter-annual variability driven by changes in precipitation and river flow, while the Detroit River load is relatively constant. Given that this modeling application treats the loads from the western basin as a combined source, reducing the load from either the Detroit or Maumee would produce a similar model response on average. However, the flow from the Detroit River is an order of magnitude greater than that of the Maumee, and therefore its flow-weighted TP concentration is much lower (Figure 11), suggesting reductions from the Maumee basin might provide the most efficient approach.

Conclusions

A 1-dimensional coupled hydrodynamic-eutrophication for the central basin of Lake Erie model has been calibrated and corroborated to in-lake data over a 19 year (1987-2005) period, during which meteorological conditions vary significantly. Applying the calibrated model to the 2008

loading time-series and simulating the response under the 19 different thermal regimes produces an envelope of expected lake response for a given TP load. Scaling the 2008 loading time-series generates response curves (Figures 3-6) that can help guide management decisions on target load reductions. For example, if managers wished to reduce the hypoxic area in the central basin to approximately 2,000 km^2, a total maximum western and central basin TP load of approximately 4800 MT would be required, representing approximately 48% reduction from the baseline 2008 loads. The load from the two dominant tributaries (Detroit and Maumee Rivers) are approximately equal (Figure 10), and therefore the required reduction should be focused on these sources. However, because the nutrient concentration in the agriculturally dominated Maumee basin are far greater, it suggests management practices in the Maumee River basin would provide the greatest benefit to reducing hypoxia in Lake Erie.

While the 48% reduction used in the illustrative example above would result in an average expected hypoxic area of 2000 km^2, variation in meteorology will also determine the level of hypoxia in any given year, as illustrated by the error bars in the response curves (Figures 3-6), variance statistics, and relationship to hypolimnion thickness (Figure 8). In addition, a warming climate is expected in the Great Lakes region in the future (Karl et al. 2009, Hayhoe et al., 2010), and this will likely lead to early and more prolonged stratification. Future climate change may lead to lower water levels as well (Angel and Kunkel, 2010) causing a thinner hypolimnion and producing greater than average hypoxia for a given load (Figure 8). These changes in the region may result in unexpected ecosystem responses, and therefore require a systematic adaptive management approach for Lake Erie load management.

Acknowledgments

This research was funded in part by the University of Michigan Graham Sustainability Institute and the USEPA under contract EP-R5-11-07, Task Order 21. The authors would like to thank Environment Canada: Water Science & Technology Branch, the EPA Great Lakes National Program Office, and NOAA-GLERL for sharing water quality data. This is NOAA GLERL contribution number XXX.

References

Angel, J.R., and K.E. Kunkel, 2010. The response of Great Lakes water levels to future climate scenarios with an emphasis on Lake Michigan-Huron. Journal of Great Lakes Research 36 Supplement 2: 51–58

Borsuk, M., Higdon, D., Stow, C. and Reckhow, K. 2001. A Bayesian hierarchical model to predict benthic oxygen demand from organic matter loading in estuaries and coastal zones. Ecological Modelling 143:165–181.

Burns, N. M., Rockwell, D. M., Bertram, P. E., Dolan, D. M., and Ciborowski, J. J. H. 2005. Trends in Temperature, Secchi Depth, and Dissolved Oxygen Depletion Rates in the Central Basin of Lake Erie, 1983-2002. Journal of Great Lakes Research 31:35-49.

Dolan, D. M. 1993. Point source loadings of phosphorus to Lake Erie: 1986-1990. Journal of Great Lakes Research 19:212-223.

Dolan, D.M., and McGunagle, K.P., 2005. Lake Erie total phosphorus loading analysis and update: 1996–2002. J. Great Lakes Res. 31 (Suppl. 2), 11–22

ECWSTB (Environment Canada, Water Science & Technology Branch) ftp:// charon.cciw.ca (accessed June 2007)

IFYLE 2006. NOAA Great Lakes Environmental Research Laboratory: International Field Years on Lake Erie (IFYLE). http://www.glerl.noaa.gov/ifyle/ 11/12/2006.GLNPO (Great Lake National Program Office. http://cdx.epa.gov/ (accessed February 2007).

GLWQA 1978. Great Lakes Water Quality Agreement.

Hayhoe, K., J. VanDorn, T. Croley II, N. Schlegal, and D. Wuebbles, 2010. Regional climate change projections for Chicago and the Great Lakes. Journal of Great Lakes Research 36 Supplement 2: 7-21.

Karl, T.R., Melillo, J., and Peterson, T.C. (eds.) 2009. Global Climate Change Impacts in the United States. Cambridge University Press.

IJC (International Joint Commission) 2012. Great Lakes Water Quality Protocol of 2012

IJC (International Joint Commission) 2014. A Balanced Diet for Lake Erie: Reducing Phosphorus Loadings and Harmful Algal Blooms. Report of the Lake Erie Ecosystem Priority

Lesht, B.M., Fontaine, T.D., Dolan, D.M., 1991. Great Lakes total phosphorus model: post-audit and regionalized sensitivity analysis. Journal of Great Lakes Research 17 (1), 3–17.

Richards, R. P. 2006. Trends in sediment and nutrients in major Lake Erie tributaries, 1975-2004. In Lake Erie Lakewide Management Plan 2006 Update pp. 22.

Richards, R. P. and Baker, D. B. 2002. Trends in water quality in LEASEQ rivers and streams, 1975-1995. Journal of Environmental Quality 31:90-96.

Rucinski, D. K., D. Beletsky, J.V. DePinto, D.J. Schwab, and D. Scavia. 2010. A simple 1-dimensional, climate based dissolved oxygen model for the central basin of Lake Erie. Journal of Great Lakes Research, 36:465-476.

Rucinski, D.K., D. Scavia, J.V. DePinto, D. Beletsky. 2014. Modeling Lake Erie's hypoxia response to nutrient loads and meteorological variability. Journal of Great Lakes Research. 40(3):151-161

Scavia, D., J.D. Allan, K.K. Arend, S. Bartell, D. Beletsky, N.S. Bosch, S.B. Brandt, R.D. Briland, I. Daloglu, J.V. DePinto, D.M. Dolan, M.A. Evans, T.M. Farner, D. Goto, H. Han, T.O. Hook, R. Knight, S.A. Ludsin, D.M. Mason, A.M. Michalak, R.P. Richards, J.J. Roberts, D.K. Rucinski, E.S. Rutherford, D.J. Schwab, T. Sesterhenn, H. Zhang, and Y. Zhou. Assessing and addressing the re-eutrophication of Lake Erie: Central basin hypoxia. Journal of Great Lakes Research 40(2):226-246

Scavia, D., DePinto, J.V., Bertani. 2016. Annex 4 multiple modeling synthesis. Journal of Great Lakes Research (this issue).

Verhamme, Edward, Todd M. Redder, Derek Schlea, Jeremy Grush, John F. Bratton, Joseph V. DePinto. 2016. Development of the Western Lake Erie Ecosystem Model (WLEEM): Application to Connect Phosphorus Loads to Cyanobacteria Biomass. Submitted to Journal of Great Lakes Research.

Zhou, Y., Obenour, D.R., Scavia, D., Johengen, T.H. and Michalak, A.M., 2013. Spatial and Temporal Trends in Lake Erie Hypoxia, 1987-2007. Environ Sci Technol. 47, 899-905.

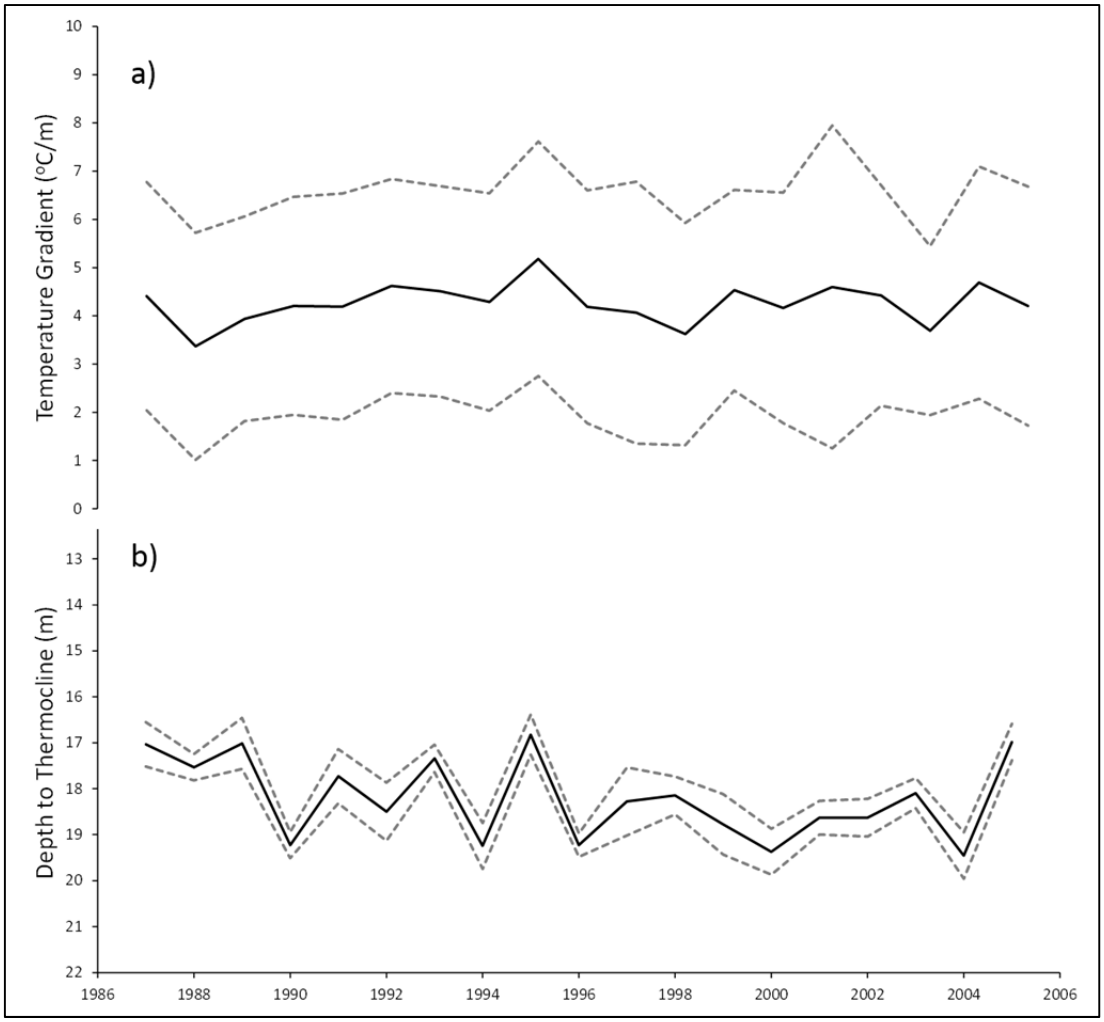

Figure 1: Interannual variation in a) temperature gradient across the thermocline and b) depth the thermocline. Mean August values shown as solid black lines, +/- 1 s.d. shown as dotted lines.

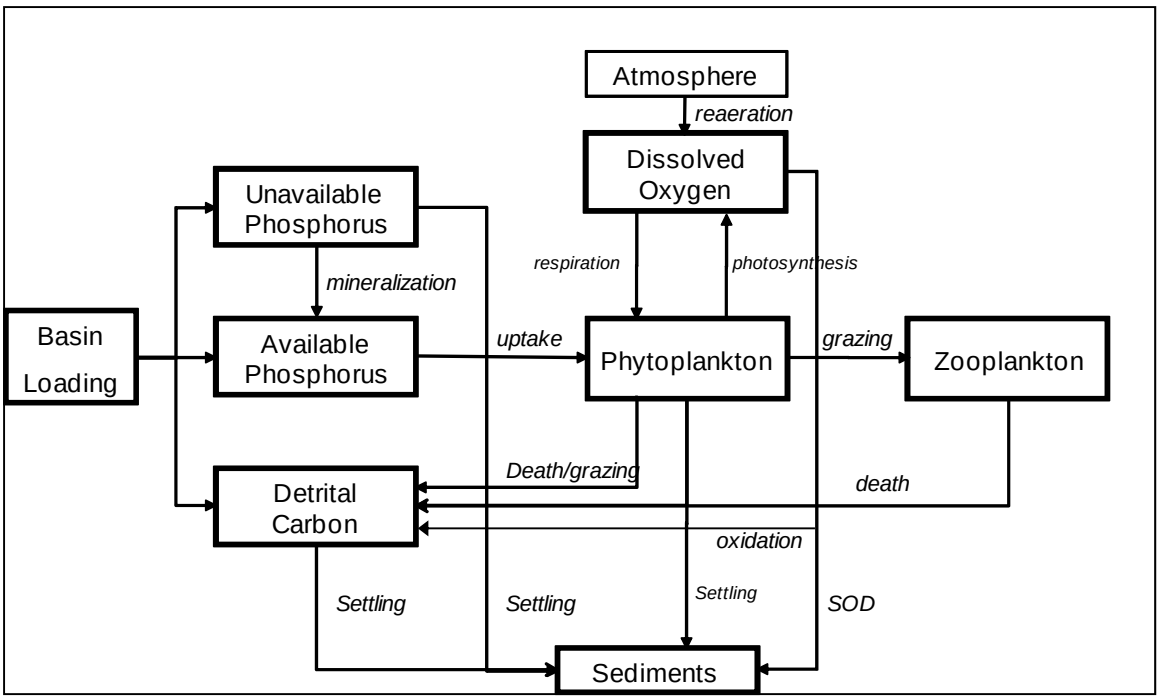

Figure 2: Conceptual diagram of eutrophication portion of the 1D Central Basin Hypoxia Model.

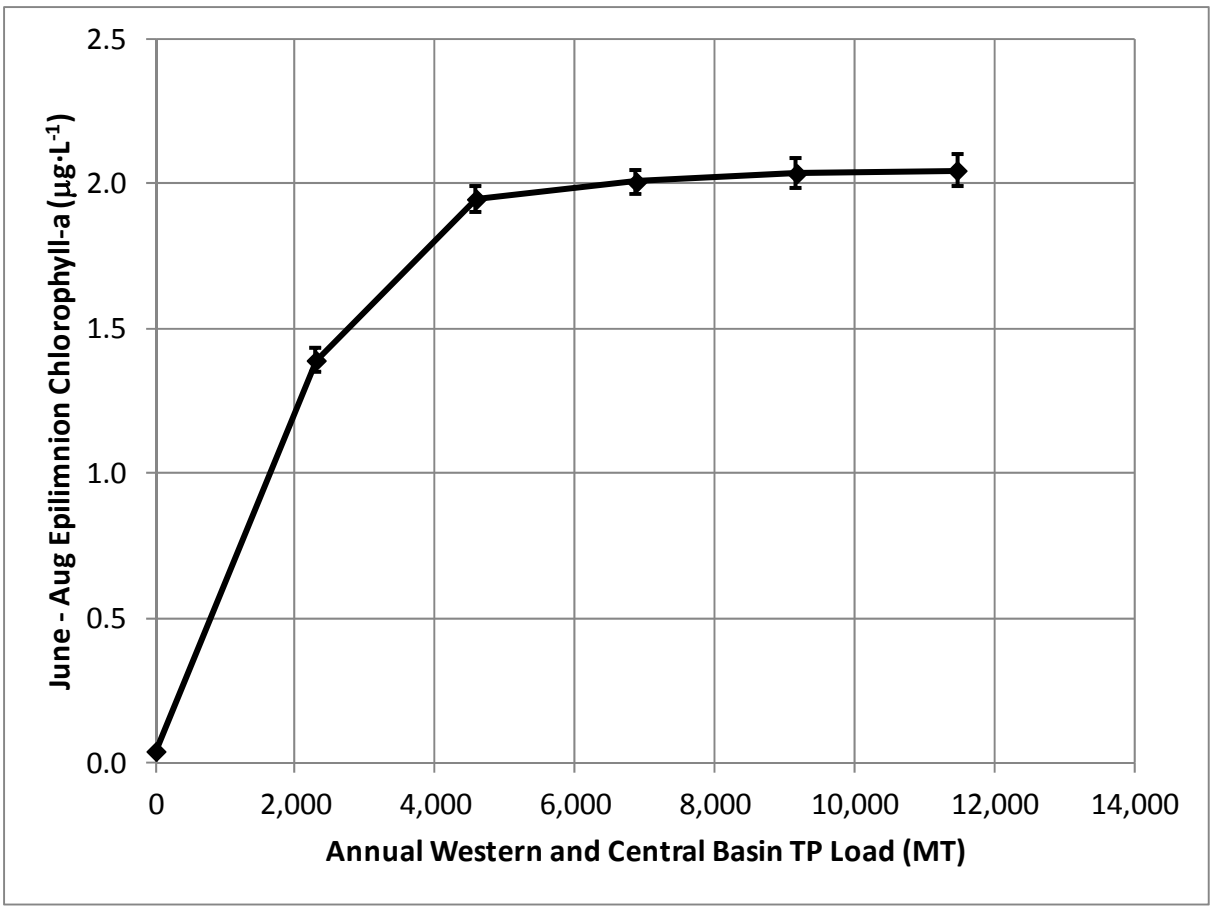

Figure 3: June – August epilimnion average chlorophyll-a load-response curve. Mean of 1987-2005 model estimates values shown as diamonds. Standard deviation of 1987-2005 values shown as vertical error bars.

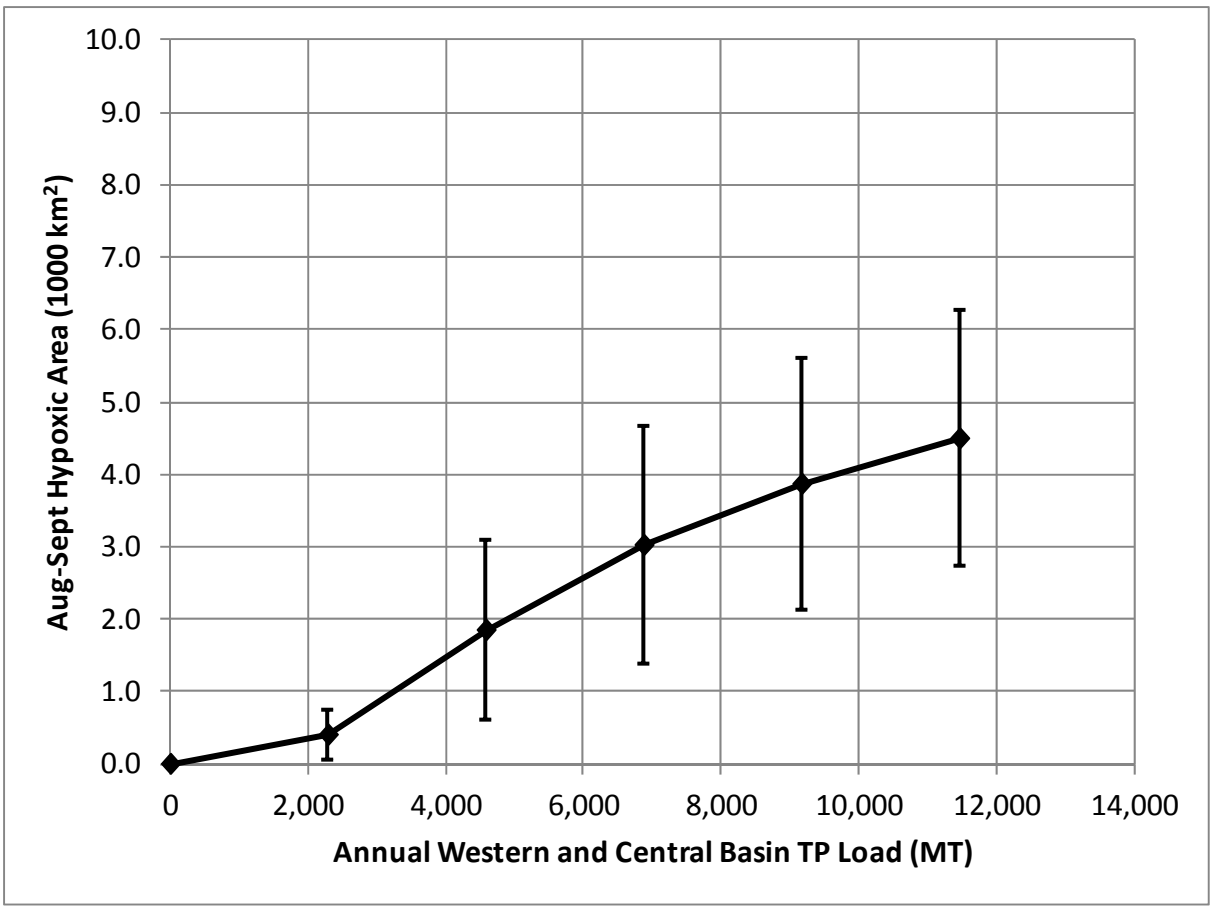

Figure 4: Aug-Sept average hypoxic area load-response curve. Mean of 1987-2005 model estimates values shown as diamonds. Standard deviation of 1987-2005 values shown as vertical error bars

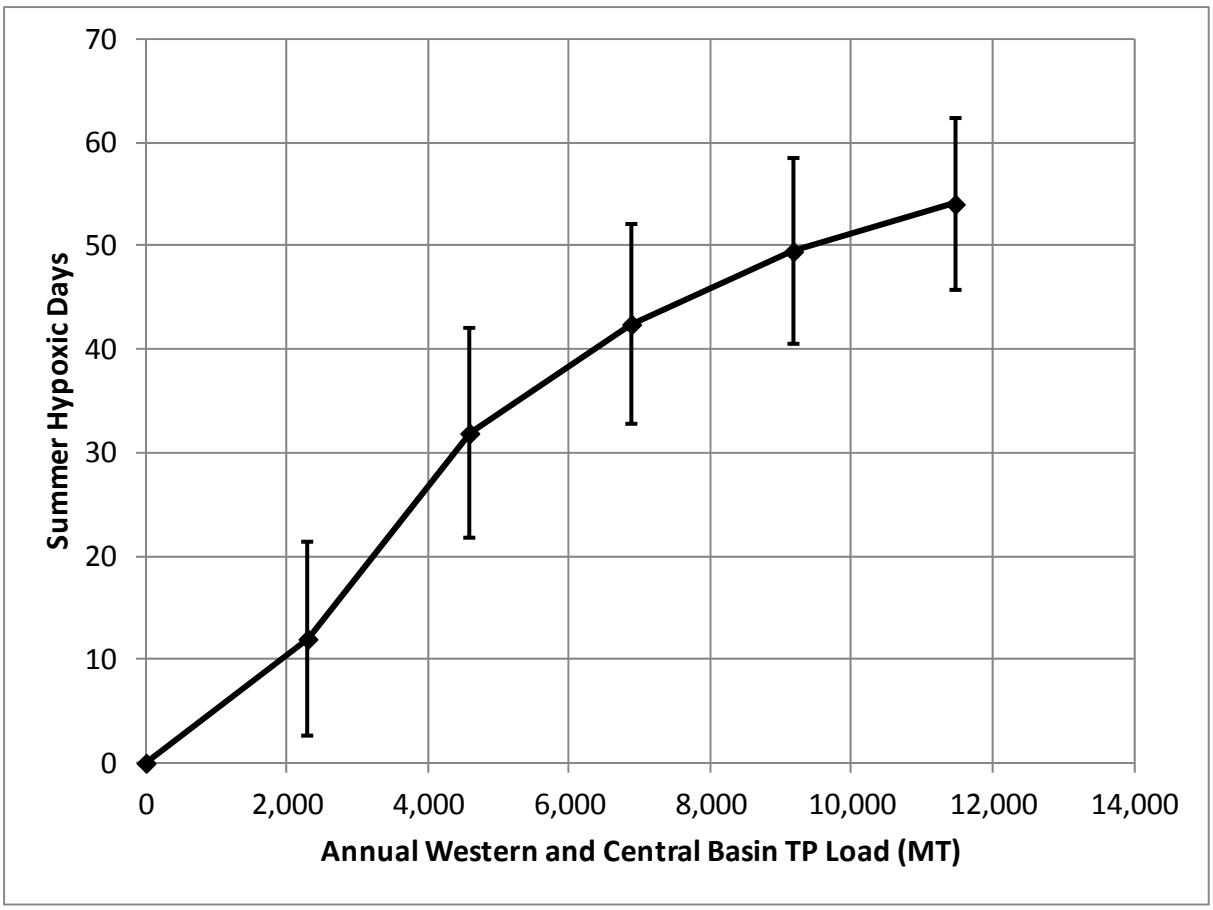

Figure 5: Number of hypoxic days load-response curve. Mean of 1987-2005 model estimates values shown as diamonds. Standard deviation of 1987-2005 values shown as vertical error bars.

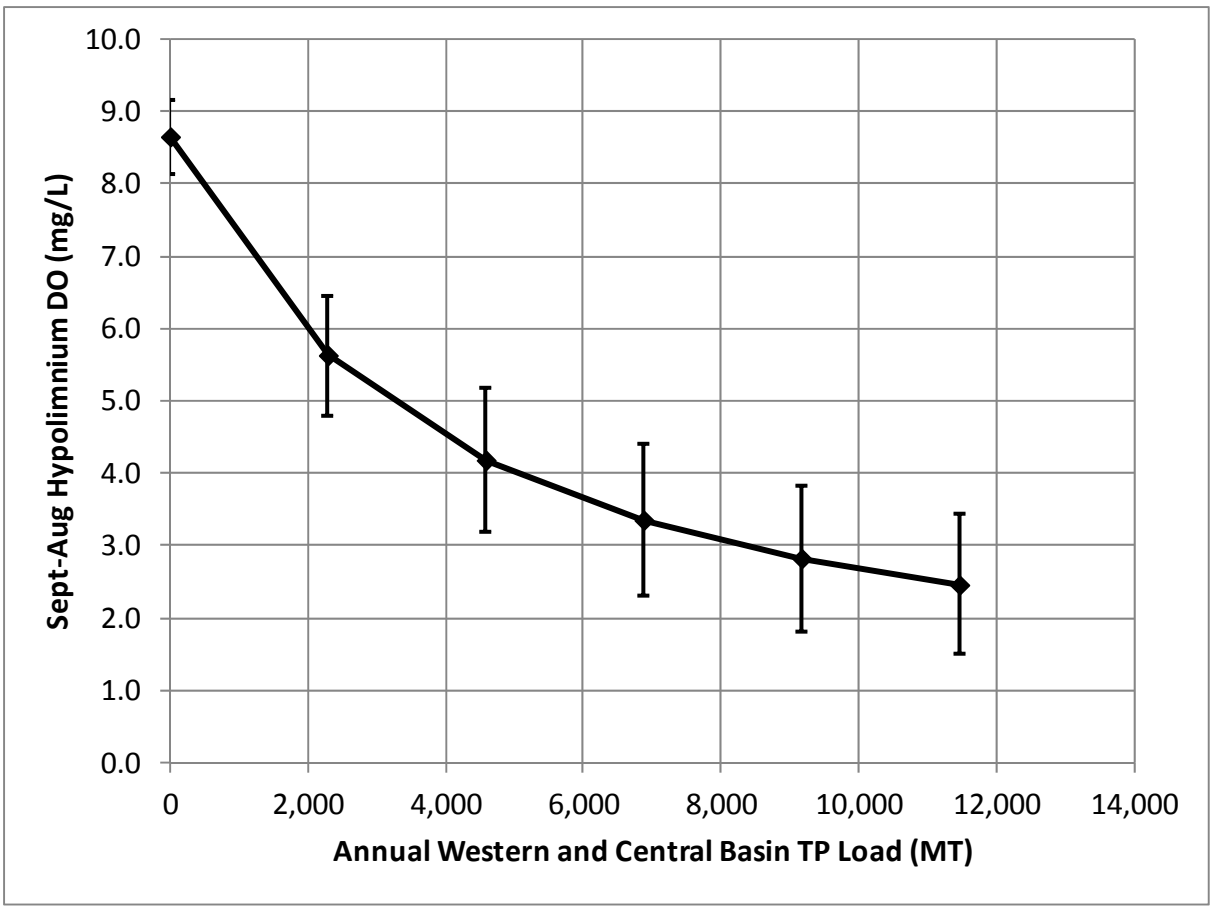

Figure 6: Aug-Sept average bottom water dissolved oxygen load-response curve. Mean of 1987-2005 model estimates values shown as diamonds. Standard deviation of 1987-2005 values shown as vertical error bars.

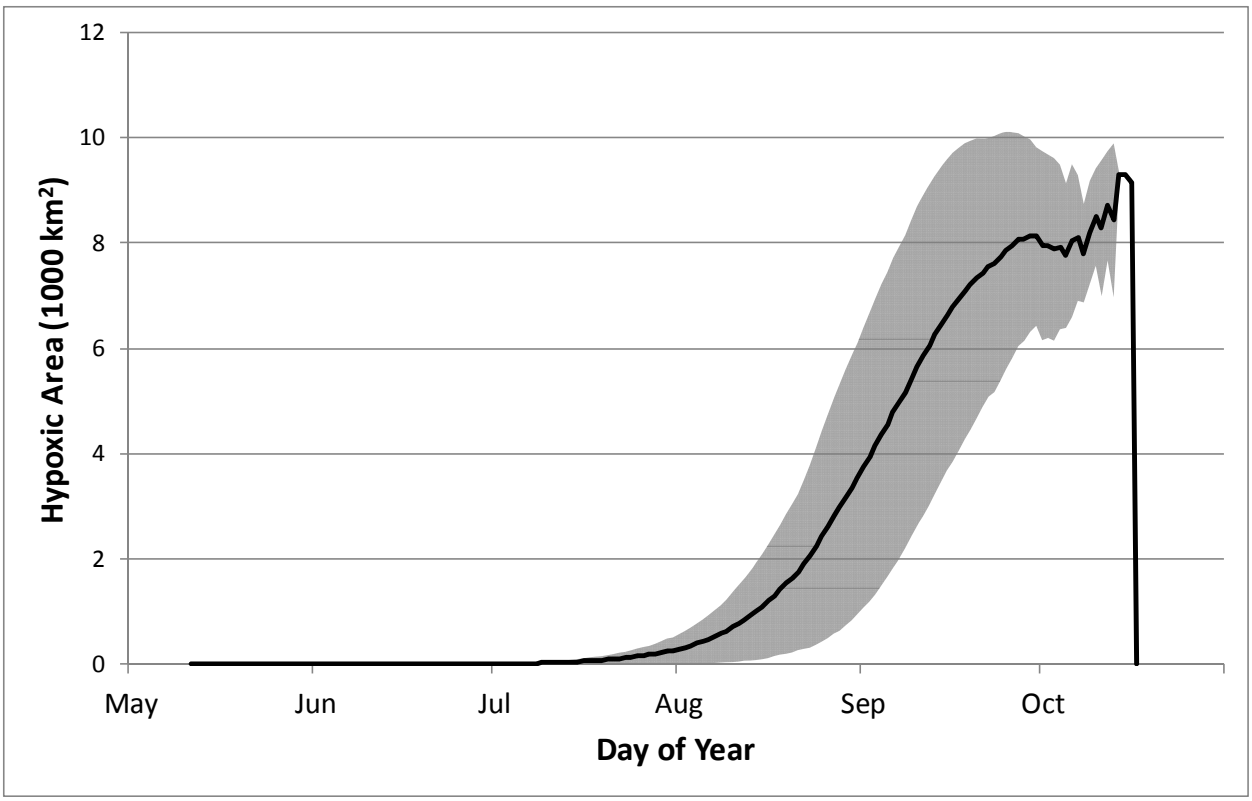

Figure 7: Temporal evolution of hypoxic extent. Mean of 1987-2005 model estimates values shown as solid line. Standard deviation of 1987-2005 values shown as shaded area.

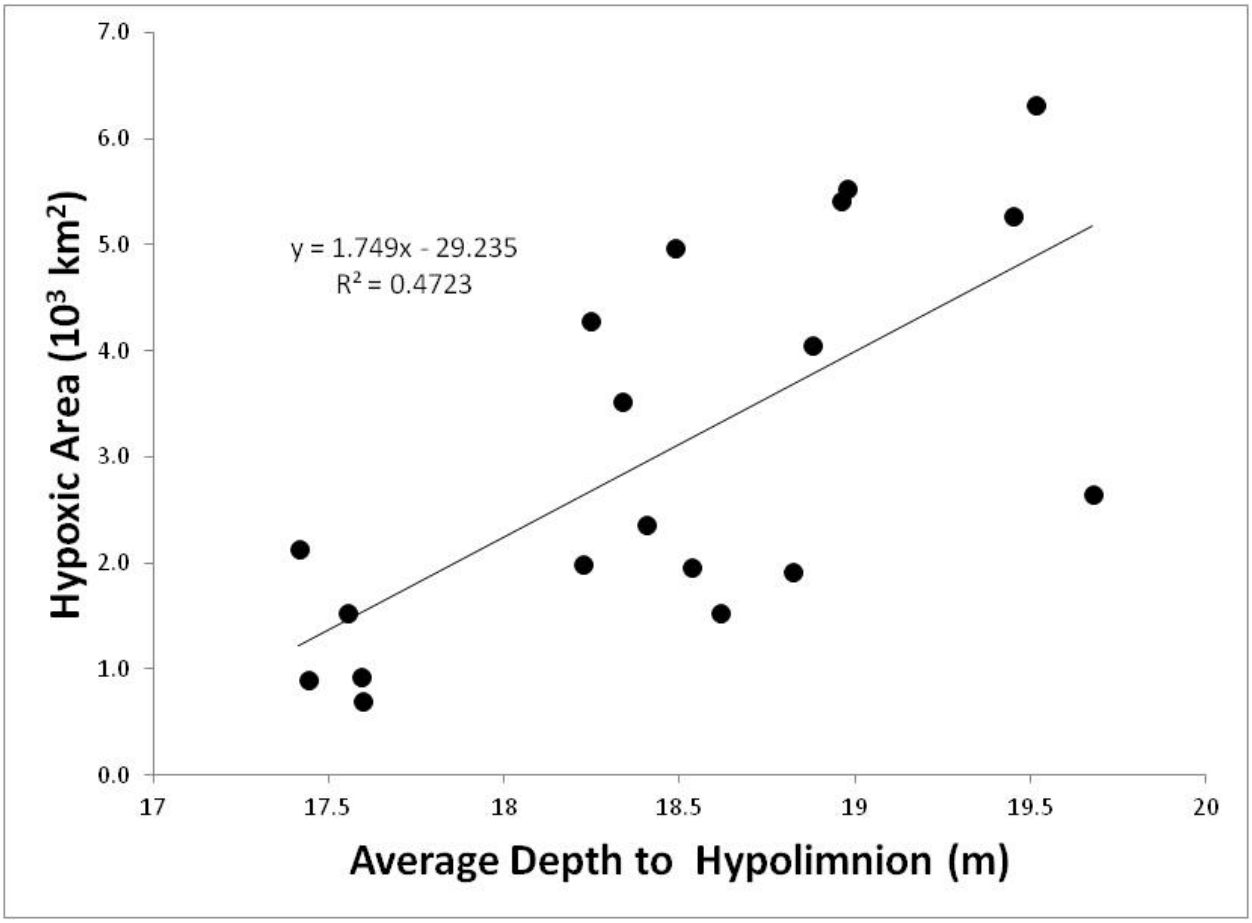

Figure 8: Comparison of September-August hypoxic area response and average depth to the hypolimnion.

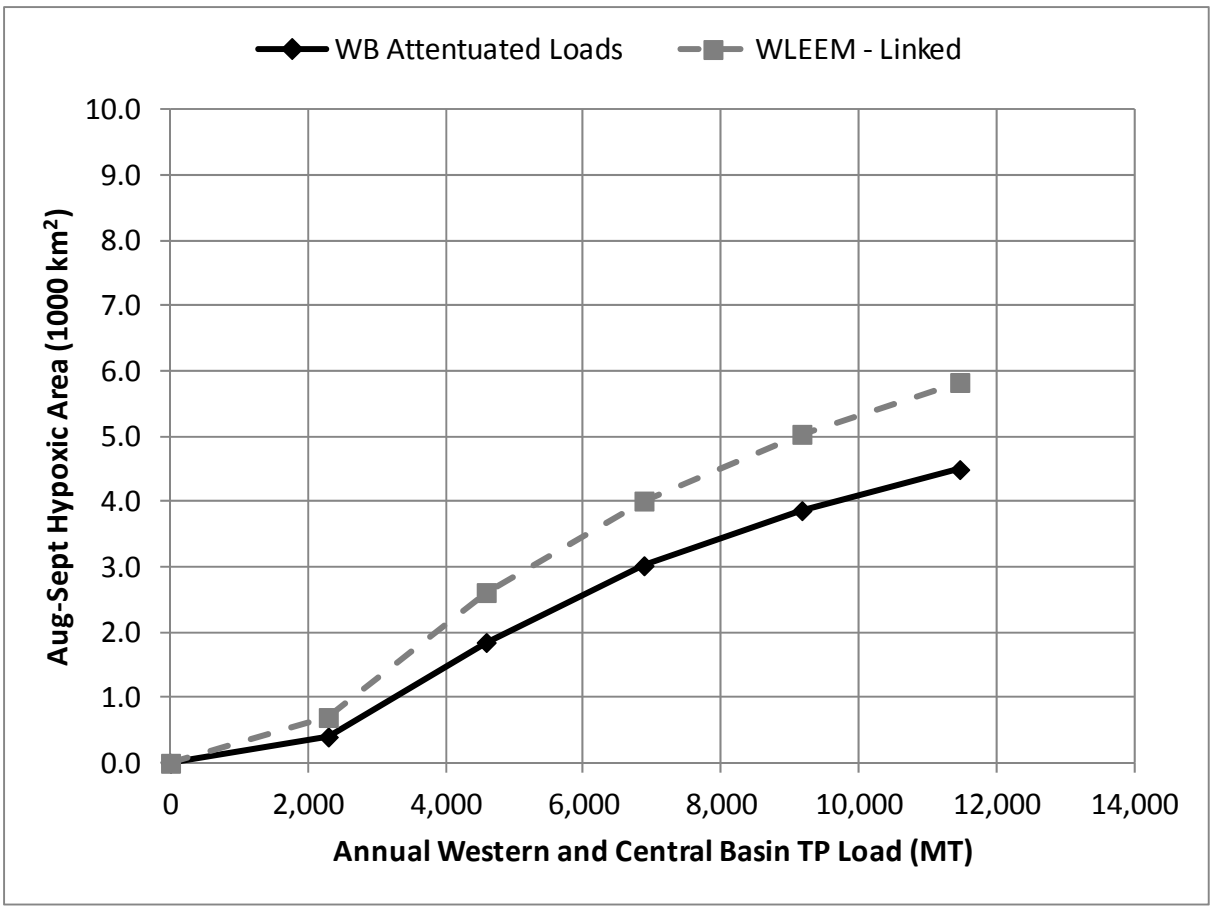

Figure 9: Comparison the hypoxic area load-response curves obtained from original model configuration (solid), and using loads from WLEEM (dashed).

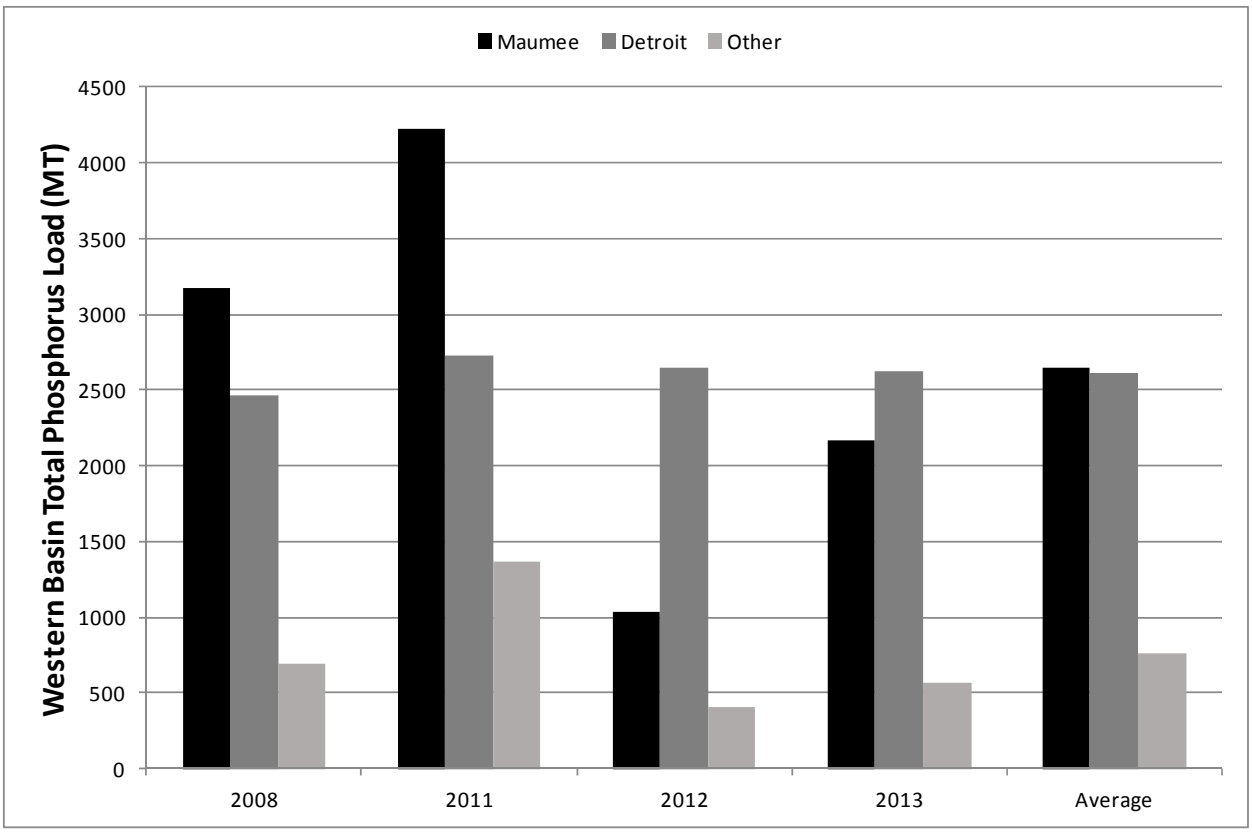

Figure 10: Annual comparison of TP load from major tributaries to western basin of Lake Erie (Maumee River: black, Detroit River: dark gray, other tributaries: light gray)

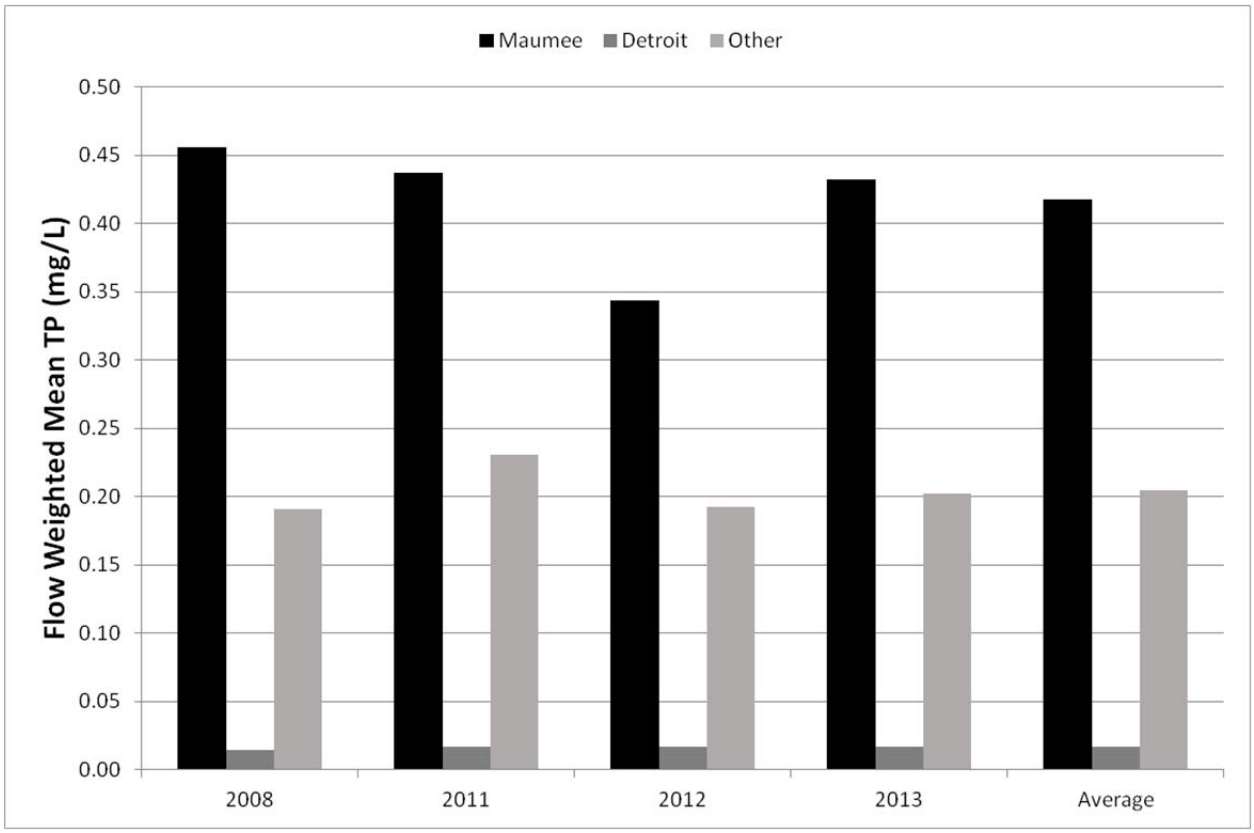

Figure 11: Annual comparison of flow-weighted mean TP concentration from major tributaries to western basin of Lake Erie (Maumee River: black, Detroit River: dark gray, other tributaries: light gray)